Environmental Science and Pollution Research (2024) 31:50857–50873
https://doi.org/10.1007/s11356-024-34496-z

RESEARCH ARTICLE

Adsorption and ion exchange of toxic metals by Brazilian clays: clay selection and studies of equilibrium, thermodynamics, and binary ion exchange modeling

Thiago Lopes da Silva[1] · Talles Barcelos da Costa[1] · Henrique Santana de Carvalho Neves[1] · Meuris Gurgel Carlos da Silva[1] · Reginaldo Guirardello[1] · Melissa Gurgel Adeodato Vieira[1]

Received: 30 April 2024 / Accepted: 22 July 2024 / Published online: 5 August 2024

Abstract

In this study, four Brazilian clays (Bofe, Verde-lodo, commercial Fluidgel, and expanded commercial vermiculite) were evaluated for their adsorptive capacity and removal percentage in relation to different toxic metals (Ni^{2+}, Cd^{2+}, Zn^{2+}, and Cu^{2+}). The best results were obtained by expanded vermiculite, with cadmium removal reaching values of 95%. The most promising clay was modified by the sodification process, and the metal cadmium was used to evaluate the ion exchange process. The clays expanded vermiculite (EV) and VNa-sodified vermiculite were evaluated by equilibrium study at 25, 35, and 45 °C. At 25 °C, EV obtained a maximum adsorption capacity of 0.368 mmol/g and sodified vermiculite 0.480 mmol/g, which represents an improvement of 30.4% in modified clay capacity. At 45 °C, the sodified vermiculite reached 0.970 mmol/g adsorption capacity. The Langmuir, Redlich-Peterson Freundlich, and Dubinin-Raduskevich models were adjusted to the results. Langmuir provided the best fit among the models. The thermodynamic quantities (ΔS, ΔH, and ΔG) demonstrated that the process is spontaneous and endothermic and the metal is captured by physisorption and chemisorption in the studied temperature range. For the ion exchange equilibrium, the binary Langmuir and binary Langmuir–Freundlich models were adjusted to the expanded vermiculite and sodified vermiculite isotherms, respectively. Both models were predictive. Thermal analysis indicated good heat resistance even after material modification. The apparent and real densities demonstrated that after each treatment or contamination, the clayey material undergoes contraction in its structure. An improved efficiency of the adsorbent was found after sodification.

Keywords Brazilian clay · Adsorption · Ion exchange · Vermiculite · Heavy metal

Introduction

Concern about the contamination of surface waters is a current issue and represents a global challenge. An estimated 2.2 billion people lack access to safely obtained potable water (WHO 2017). Population growth, urban expansion, and industrialization imply the use and disposal of a series of contaminants that deteriorate the quality of surface water, which will later be used for human consumption.

Inorganic contaminants, such as toxic metals, represent a concerning class of substances due to the detrimental effects they exert on the environment and human health. These substances accumulate in the body and, even in low concentrations, can lead to the development of cancers and mutagenic processes. The most representative metals include lead, zinc, chromium, cadmium, copper, arsenic, nickel, and mercury. The release of these metals includes compounds discharged by modern chemical industries, galvanizing companies, pesticides, fertilizers, batteries, leather, paints, dyes, dye-fixing agents in textile fibers and mordants, mining waste, and metal alloy processing residues, among many other metal-containing contaminant compounds (Park et al. 2019; Fiyadh et al. 2019; Wadhawan et al. 2020; Rajendran et al. 2022).

Responsible Editor: Guilherme Luiz Dotto

Thiago Lopes da Silva and Talles Barcelos da Costa equally contributed to this study as first authors.

✉ Melissa Gurgel Adeodato Vieira
melissag@unicamp.br

[1] School of Chemical Engineering, University of Campinas, Av. Albert Einstein, 500, Campinas, São Paulo 13083-852, Brazil

Among the toxic metals, cadmium stands out for its high toxicity. This metal can cause pulmonary fibrosis, dyspnea, chronic lung disease, testicular degeneration, and kidney and liver disorders, besides being carcinogenic (Ahmaruzzaman 2011; Neves et al. 2022).

Among the methods used in the treatment of liquids contaminated with toxic metals, adsorption is considered a suitable method for the toxic metal removal due to its efficiency, even when contaminants are in low concentrations and low energy consumption, and the possibility of using waste and alternative, sustainable, and low-cost materials as efficient adsorbents, like clays (Fiyadh et al. 2019; Silva et al. 2021; Neves et al. 2022).

Clays have important characteristics such as low cost, abundance, high adsorption capacity, high cation exchange capacity (CEC), and the possibility of being physically and chemically modified to obtain better adsorption properties on clay minerals (Ngah and Hanafiah 2008). de Farias et al. (2022b) present some physical and chemical modifications that can be applied to clays to increase the sorption capacity of organic and inorganic contaminants, such as calcination, acid and alkaline treatment, and modification with surfactants. Modified clays in adsorption studies are a current topic and some works can be cited: Cd^{2+} adsorption in clay-microbe aggregates (Zhou et al. 2020), organic clay associations (12-aminododecanoic acid and montmorillonite) (Xu et al. 2022) and Moroccan clays (QC-MC and QC-MC) (Bassam et al. 2021), Pb^{2+} and Hg^{2+} in Romanian clay (Azamfire et al. 2020), Cr^{3+} in montmorillonite (Essebaai et al. 2022), Cd^{2+} and Pb^{2+} on sodified Fluidgel® clay (Galindo et al. 2013), Ag^{+} and Cu^{2+} on Verde-lodo bentonite (Cantuaria et al. 2015, 2016; Freitas et al. 2017; de Freitas et al. 2018), Ce^{3+} on alginate/modified vermiculite particles (de Farias et al. 2022a, 2023), and rare earth metals in expanded vermiculite (Brião et al. 2024), among others.

In this study, four Brazilian clays were evaluated for the removal of metal contaminants. The clays are three bentonites (Bofe, Verde-Lodo, and Fluidgel) and one vermiculite (expanded vermiculite). Bentonitic clays are mainly composed of montmorillonite, exhibiting high specific surface area and affinity for organic pollutants and some toxic metals (Khan et al. 2023). Bentonite clays consist of lamellae formed by an octahedral sheet of Al_2O_3 between two tetrahedral sheets of SiO_2. In the octahedral positions, the cations can be Al^{3+}, Mg^{2+}, or Fe^{3+}, and in the tetrahedral layer, isomorphic substitutions of Si^{4+} for Al^{3+} can occur (Antonelli et al. 2020). The USA and South Africa have the largest vermiculite reserves in the world (Paula 2014). Vermiculite, a geological denomination encompassing a group of hydrated laminar minerals, comprises aluminum-iron-magnesium silicates, bearing resemblance to mica in physical appearance (Assis Neto et al. 2023). Vermiculite clays are layered phyllosilicate minerals, classified as type 2:1, where 2 tetrahedral layers are intercalated by an octahedral layer. The tetrahedral layers, composed of SiO_4, also contain Al^{3+} and Fe^{3+} ions. The composition of the octahedral layer consists of $Al(OH)_3$ and $Mg(OH)_2$ (Neves et al. 2022). The presence of ions in the composition and between the clay layers allows ion exchange with pollutants. When heated rapidly, vermiculite undergoes exfoliation as the water within its structure vaporizes, promoting a distancing of the silicate layers (Sutcu 2015). After exfoliation, expanded vermiculite exhibits greater porosity and increased surface area and, commercially, this clay is used in civil construction as a material with thermal and acoustic insulation characteristics (Marcos and Rodríguez 2014; Neves et al. 2022).

The present work is a continuation that complements the article by Neves et al. (2022). Previously published work investigated the kinetic behavior of adsorption and ion exchange, CEC, and characterizations to understand the mechanisms involved in the adsorption process. The present work aims to evaluate the affinity of Brazilian clays for toxic metals and propose modifications to the clay to improve the adsorption properties of the solid. The most promising clay, expanded vermiculite, was subjected to the sodification modification process, to increase the mineral's ion exchange capacity. A complete adsorption equilibrium study with cadmium metal was performed and the results were investigated by single-component models (Langmuir, Freundlich, Redlich-Peterson, and Dubinin-Raduskevich) and binary predictive models (binary Langmuir and binary Langmuir–Freundlich). pH monitoring, metal speciation as a function of pH, and determination of thermodynamic parameters were also performed.

Materials and methodologies

Reagents

The reagents required to carry out the experiments were as follows: nickel nitrate, $Ni(NO_3)_2{\cdot}6H_2O$ (97.3%, Dinâmica Ltda., Brazil); cadmium nitrate, $Cd(NO_3)_2{\cdot}4H_2O$ (103.7%, Vetec, Brazil); zinc nitrate, $Zn(NO_3)_2{\cdot}6H_2O$ (99.9%, Synth, Brazil); copper nitrate, $Cu(NO_3)_2{\cdot}3H_2O$ (101.64%, Dinâmica Ltda., Brazil); nitric acid, HNO_3 (65.88%, Anhydrol, Brazil); ammonium hydroxide, NH_4OH (28%, Dinâmica Ltda., Brazil); and sodium chloride, NaCl (99.9%, Dinâmica Ltda., Brazil). Four Brazilian clays were evaluated: three bentonite clays, i.e., Bofe, Verde-Lodo, commercial Fluidgel (Dolomil, Brazil—State of Paraíba), and the commercial clay expanded vermiculite (Brasil Minérios, Brazil).

Preparation of clay materials

Initially, with the aim of selecting the most promising clay for metal removal, the bentonite clays Bofe, Fluidgel,

Verde-lodo and expanded vermiculite were evaluated for their adsorptive affinity against four metals: nickel (Ni^{2+}), cadmium (Cd^{2+}), zinc (Zn^{2+}), and copper (Cu^{2+}). The bentonite clays were ground, using a manual coffee grinder, and calcined at 500 °C for 24 h, to enhance the stability of the adsorbent. Subsequently, the clays were sieved until reaching an average particle diameter of 0.855 mm. Commercially, expanded vermiculite is produced by rapid heating (850 °C), which causes the expulsion of water and expansion of the mineral layers. Due to this production process, expanded vermiculite (EV) did not undergo calcination, unlike bentonite clays. The preparation of expanded vermiculite involves crushing the material, sieving, and drying at 105 °C for 24 h.

The results indicated that expanded vermiculite was the most promising in the adsorptive affinity tests. Therefore, aiming to evaluate the removal mechanism by ion exchange, this selected adsorbent was sodified; that is, it received a treatment with sodium in an acidic medium. To modify the clay with sodium, the procedure consisted of immersing the adsorbent in a 1% NaCl acidified solution (pH 3 using 0.1 mol/L nitric acid), under agitation (120 rpm) for 3 h (Almeida Neto et al. 2014). The proportion used was 10 g of adsorbent per 1 L of solution (NaCl, 1% w/v, pH 3). After treatment, the clay was rinsed with 4 L of deionized water (filter paper). After washing, the sodium concentration in the filtrate should be zero, which indicates that the metal not bonded to the surface has been all removed. Finally, the clay was dried at 105 °C (24 h) and sieved (dp = 0.885 mm) to be used in this study. In this work, expanded vermiculite clay and sodified vermiculite clay are referred to as EV and VNa, respectively.

Metal speciation for pH selection

Diagrams of metal speciation as a function of the pH were used to select the pH of the experiments. The Hydra database and the Medusa software were used to obtain the metallic speciation diagrams (Puigdomenech 2010). In the simulation, the concentrations of all reagents used (nitrates) were provided and the results indicate which ionic forms are present and the minimum pH at which ion precipitation occurs. This analysis is an estimate, as the ions released by the adsorbents during the experiment are not taken into account. However, it is widely used in adsorption studies to establish a pH range in which only adsorption and not chemical precipitation is responsible for decreasing the target ion concentration.

Clay selection—evaluation of metal removal by clays (adsorptive affinity tests)

Four Brazilian clays were evaluated for their performance in removing toxic metals. The affinity tests were carried out with four clays, i.e., three bentonite clays (Bofe, Verde-lodo, Fluidgel) and a vermiculite clay (commercial expanded vermiculite), and four toxic ions, i.e., Ni^{2+}, Cd^{2+}, Zn^{2+}, and Cu^{2+} in monocomponent solutions of 1 mmol/L. In total, 16 different experiments were carried out. Through speciation analysis (Hydra/Medusa), it was observed that the maximum pH is 5; that is, from this value onwards, metal precipitation in solution occurs. Therefore, pH 4.5 was used in the experiments, a value with a safety margin to carry out the experiments without risk of precipitation. Solutions of metallic nitrate salts were prepared with water acidified (pH 4.5) with 0.1 mol/L nitric acid.

For adsorptive affinity tests, 0.5 g of adsorbent was immersed in 50 mL of monocomponent metal solution (dosage 10 g/L). The samples were shaken in an incubator shaker (Jeio Tech-Lab. Companion SI 600R, Korea) at 25 °C, 200 rpm, for 24 h. The samples were centrifuged (3000 rpm), filtered through a syringe filter (0.45 um), and the metal concentration was measured by Atomic Absorption Spectrophotometry (Shimadzu, AA-7000, Japan). All experiments were performed in triplicate. The average deviation of the experimental curves was below 3.1%. The adsorptive capacity (q_e) (mmol/g) and removal percentage (%R) were determined with Eqs. 1 and 2.

$$q_e = \frac{(C_0 - C_e)}{m} \cdot V \tag{1}$$

$$\%R = \frac{(C_0 - C_e)}{C_0} \cdot 100 \tag{2}$$

wherein C_0 is the initial metal concentration (mmol/L), C_e is the equilibrium metal concentration (mmol/L), V is the solution volume (L), and m is the mass (g).

Due to the variation in pH in the samples during the experiment, this parameter was monitored during the clay selection tests (affinity tests). At pre-defined times, the pH was measured and adjusted, using solutions of nitric acid (0.1 mol/L) and ammonium hydroxide (0.2 mol/L), to values in the range of 4.2 to 4. 8. The collected data was used to evaluate the pH variation in adsorptive affinity tests (Fig. 2).

Equilibrium and thermodynamic study

The equilibrium study was carried out with expanded vermiculite and sodified vermiculite clays. The adsorption isotherms were evaluated at temperatures of 25, 35, and 45 °C using a shaker incubator. Each isotherm was obtained with 15 different C_0 ranging from 0.25 to 6 mmol/L. The adsorbent dosage was 10 g/L: 0.5 g of clay was placed in contact with 50 mL of metal solution in Erlenmeyer flasks and shaken (200 rpm) at constant temperature. After the equilibration time, the samples were centrifuged (3000

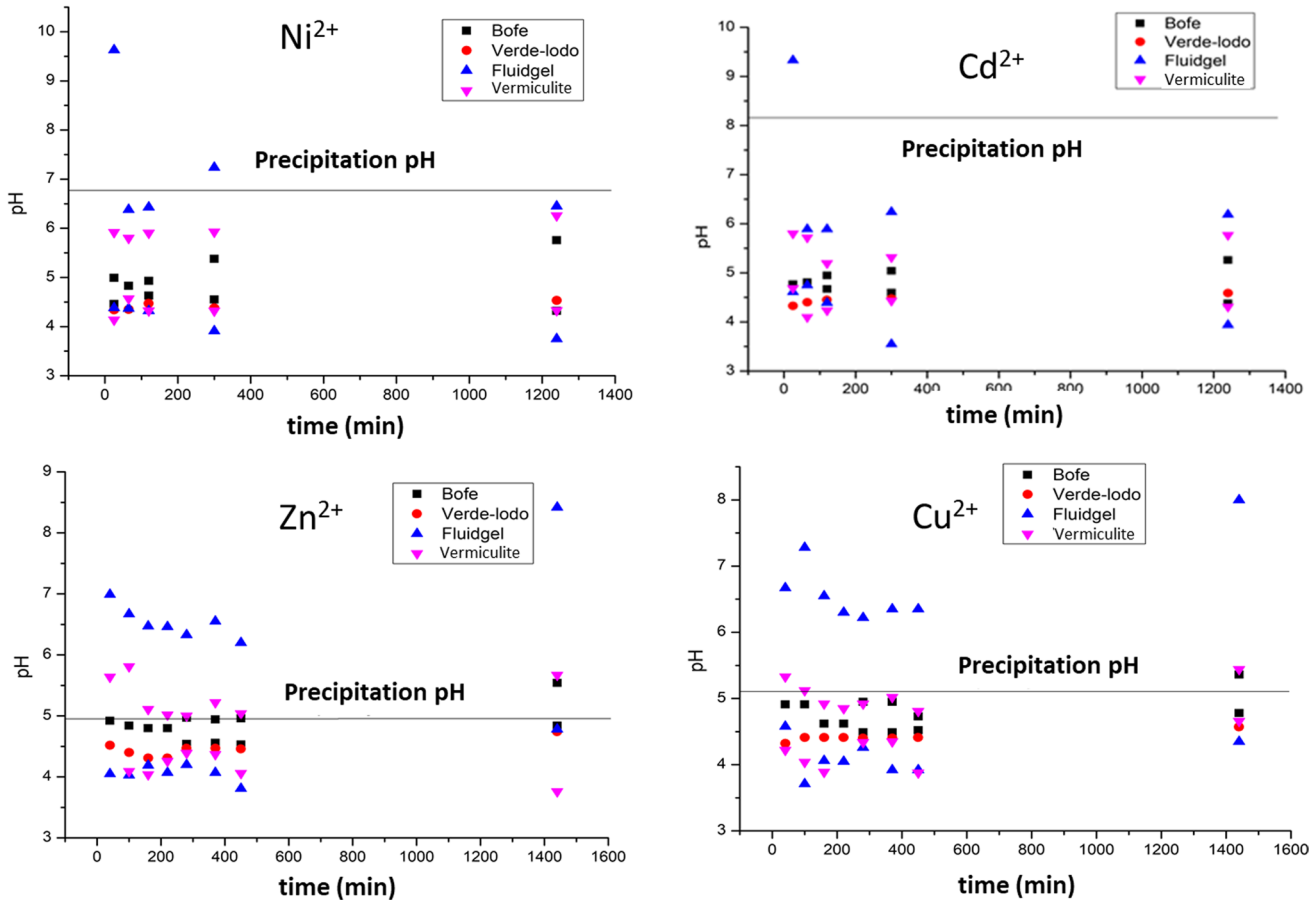

Fig. 1 pH variation in affinity tests: Ni^{2+}, Cd^{2+}, Zn^{2+} and Cu^{2+} on Bofe, Verde-lodo, Fluidgel and expanded vermiculite clays

rpm, 10 min) and filtered (syringe filter, 0.45 um) and the metal concentration was determined by atomic absorption spectrophotometry.

The Langmuir, Redlich-Peterson, Freundlich, and Dubinin-Radushkevich models (Eqs. 3–9) (Table 1) were fitted to the equilibrium data using Maple® 17 and Origin® 7.0 software.

For ion exchange equilibrium investigation, the concentration of light metals (Na^+ and Mg^{2+}) was measured. The binary Langmuir and binary Langmuir–Freundlich models (Eqs. 10–13) (Table 1) were fitted to data from systems with expanded and sodified vermiculite adsorbents, using the Solver tool in the Excel® software, which uses the GRG nonlinear algorithm.

The thermodynamic quantities (ΔG, ΔH, and ΔS) (Eqs. 14–17) were calculated by Henry's Law (Table 2) from the adjustment to the infinitely diluted region of the isotherm (lower concentrations where a linear trend is observed).

C_e equilibrium concentration (mmol/L), K_L =Langmuir isotherm constant (L/mmol), q_{max} maximum biosorption capacity of Langmuir model (mmol/g), R_L separation factor (-), K_F Freundlich isotherm constant (mmol/g) $(L/mmol)^{1/n}$, n Freundlich heterogeneity factor (-), q_m biosorption capacity of D-R isotherm (mmol/g), K_D D-R isotherm constant (mol^2/J^2), ε Polanyi potential (J/mol), R universal gas constant (J/mol·K), T temperature (K), E mean free energy of biosorption (J/mol), K_{RP} Redlich-Peterson constant (L/mmol), α_{RP} Redlich-Peterson constant (L/mmol), β_{RP} exponent of the Redlich-Peterson model (-)

ΔG Gibbs energy change (kJ/mol), ΔH enthalpy change (kJ/mol), ΔS entropy change (J/mol·K), K_C dimensionless equilibrium constant (-), ρ specific mass of water (g/L), K_d Henry's constant (L/mmol), and K'_d dimensionless Henry's constant (-)

Statistical evaluation of model fits

For statistical analysis of the models' fit to the experimental results, the parameters evaluated were the coefficient of determination (R^2) (Eq. 18), the relative mean deviation (RMD) (Eq. 19), and the corrected value of Akaike information criterion ($AICc$), calculated by Eq. 20 (Bonate and Steimer 2011; Rahman and Sathasivam 2015).

Table 1 Isothermal models of monocomponent and binary adsorption

	Models	Equations		References
Monocomponent models	Langmuir	$q_e = \frac{K_L q_{max} C_e}{1+K_L C_e}$	(3)	Langmuir (1918)
		$R_L = \frac{1}{1+K_L C_0}$	(4)	
	Freundlich	$q_e = K_F C_e^{1/n}$	(5)	Freundlich (1906)
	Dubinin-Radushkevich	$q_e = q_m \exp(-K_D \varepsilon^2)$	(6)	Dubinin and Radushkevich (1947)
		$\varepsilon = RT\ln\left(1 + \frac{1}{C_e}\right)$	(7)	
		$E = \left(2K_D\right)^{-0.5}$	(8)	
	Redlich-Peterson	$q_e = \frac{K_{RP} C_e}{1+a_{RP} C_e^{\beta_{RP}}}$	(9)	Febrianto et al. (2009)
Binary models	Binary Langmuir	$q_{e,A} = \frac{q_{A(max)} K_{L,A} C_{e,A}}{1+K_{L,A} C_{e,A}+K_{L,B} C_{e,B}}$	(10)	Ruthven (1984)
		$q_{e,B} = \frac{q_{B(max)} K_{L,B} C_{e,B}}{1+K_{L,A} C_{e,A}+K_{L,B} C_{e,B}}$	(11)	
	Binary Langmuir–Freundlich	$q_{e,A} = \frac{q_{A(\max)} K_{L,A} (C_{e,A})^{K_A}}{1+K_{L,A} (C_{e,A})^{K_A}+K_{L,B} (C_{e,B})^{K_B}}$	(12)	
		$q_{e,B} = \frac{q_{B(\max)} K_{L,B} (C_{e,B})^{K_B}}{1+K_{L,B} (C_{e,B})^{K_B}+K_{L,A} (C_{e,A})^{K_A}}$	(13)	

Table 2 Thermodynamic parameters

Equations		Reference
$\Delta G = -R \cdot T \cdot lnK_C$	(14)	Tran et al. (2016)
$\Delta G = \Delta H - T \cdot \Delta S$	(15)	
$lnK_C = -\frac{\Delta H}{R \cdot T} + \frac{\Delta S}{R}$	(16)	
$K_d = \frac{q_e}{C_e}, K\prime_d = K_d[L/mmol] \cdot \rho[mmol/L]$	(17)	

$$R^2 = \frac{\sum_{i=1}^{N}(q_{i,calc} - \overline{q_{exp}})^2}{\sum_{i=1}^{N}(q_{i,exp} - \overline{q_{exp}})^2} \tag{18}$$

$$RMD(\%) = \frac{\sum_{i=1}^{N}\left|\frac{q_{i,calc}-q_{i,exp}}{q_{i,exp}}\right|}{N}.100 \tag{19}$$

$$AIC_c = N.\ln\left(\sum_{i=1}^{N}\frac{\left(q_{i,exp} - q_{i,calc}\right)^2}{N}\right) + 2p + \frac{2p(p+1)}{N-p-1} \tag{20}$$

where N is the number of experimental points, $q_{i,exp}$ is the experimental value of the sample of point i, $q_{i,calc}$ is the estimated value of the model for the sample of point i, and p is the number of parameters + 1 (variance component).

The *AICc* for small samples is used to compare different models regarding their fits to experimental data. The lower the *AICc* value among the models, the better their performance in predicting the experimental data (Bonate and Steimer 2011; Silva et al. 2021).

For ion exchange equilibrium, it is necessary to fit the models to Cd^{2+} and light metal concentration data in the solid phase simultaneously. This fitting was achieved by minimizing the objective function (F_{obj}) represented by Eq. 21.

$$F_{obj} = \sum_{i=1}^{N}\left[\left(q_{Cd,i}^{calc} - q_{Cd,i}^{exp}\right)^2 + \left(q_{LM,i}^{calc} - q_{LM,i}^{exp}\right)^2\right] \tag{21}$$

where $\boldsymbol{q_{Cd,i}^{calc}}$ and $\boldsymbol{q_{Cd,i}^{calc}}$ are the adsorption capacities (mmol/g) of Cd^{2+} calculated by the model and experimental, respectively; $\boldsymbol{q_{LM,i}^{calc}}$ and $\boldsymbol{q_{LM,i}^{exp}}$ are the solid-phase concentrations of the light metal (LM = Mg or Na) calculated by the model and experimental, respectively.

Characterization of adsorbent solids

The characterization of the adsorbents, expanded and sodified vermiculite, before and after the adsorption of Cd^{2+} ions, was carried out to understand the thermal and structural properties of the materials. The techniques used for characterization were thermogravimetry (TG), mercury porosimetry, and helium gas pycnometry (Table 3).

With the values of the real density and apparent density, it is possible to calculate the porosity of the adsorbent solid using Eq. 22.

$$\varepsilon_p = 1 - (\rho_{\text{apparent}}/\rho_{\text{real}}) \tag{22}$$

wherein ε_p is the particle porosity, ρ_{apparent} is the apparent density obtained by mercury porosimetry, and ρ_{real} is the real (true) density obtained by helium gas picnometry.

Table 3 Vermiculite characterization analyses

Analysis	Objective	Operating conditions	Equipment
Thermogravimetry	Evaluate thermal stability	Air flow: 50 mL/min of N_2; heating ratio 10 ℃/min; T = 25 to 1000 ℃	TGA–50, Shimadzu
Mercury porosimetry	Determine the apparent density	Mercury intrusion pressure: 0.5 and 60,000 psia; evacuation pressure of 50 µmHg, evacuation time of 5 min and equilibrium time of 10 s	AutoPore IV Mercury Porosimeter Micromeritics
Helium gas pycnometry	Determine the real density	T = 28 ℃; equilibrium ratio 0.0010 psig/min	Accupyc 1330, Micromeritics

Results and discussion

Metal speciation

From the metal speciation diagrams, it is possible to determine the pH range in which only bivalent ionic species are present. When the adsorbent comes into contact with the solution, its matrix undergoes changes due to the release of ions into the solution and ion exchange. Therefore, during the adsorption and ion exchange experiments, the pH was properly monitored. Figure 1S-1 (Supplementary Material) shows the speciation diagrams for each metal evaluated in the affinity test: Ni^{2+}, Cd^{2+}, Zn^{2+}, and Cu^{2+}, each at a concentration of 1 mmol/L.

In solutions prepared with zinc nitrate, up to pH 6.7, only the soluble ionic form of the metal is observed; from this pH onward, the formation of precipitable $Ni(OH)_2$ occurs. Thus, working at values above this pH, in adsorption and ion exchange studies, the decay of the metal concentration in the liquid medium is biased by the precipitation process; that is, adsorption and ion exchange would not be the only processes responsible for removing the metal from the solution. In solutions with cadmium nitrate, the pH limit is 8.2; with zinc nitrate, the pH is 5; and for copper nitrate, the pH is 5.1. The pH selected in the study is 5, as it is the value that meets all possible solutions studied. Therefore, the pH must remain below this value (pH 5) in experiments.

Based on the speciation results, the use of acidified water (at pH 4.5) was standardized to prepare the solutions used in the affinity tests. During the tests, the pH was monitored and corrected to values in the range between 4.2 and 4.8. In this pH range, all metals investigated are in divalent ionic form.

Adsorptive affinity tests

Adsorptive affinity tests were carried out to select the clay-metal system with the greatest removal potential. It should be noted that other factors, such as changes in the pH of the medium in contact with the clay and the ease of removing the clay suspension from the collected samples, were evaluated. In previous work (Neves et al. 2022), the kinetic evaluation of Cd^{2+} adsorption indicated that equilibrium was achieved in 45 min for EV and 10 min for VNa clays. In the present work, the affinity experiments lasted 24 h. As the kinetic evaluation was not carried out for all clays, it cannot be stated that equilibrium was reached in the systems with Bofe, Verde-Lodo, and Fluidgel clays. Although 24 h is a long time and equilibrium has likely been reached for all systems (especially since clays typically do not exhibit slow kinetics for metal adsorption), we considered here that the q values represent the adsorption capacity of clays over 24 h.

Table 4 shows the values of the adsorptive removal percentages and the adsorbed amount of the different ions by the clays assessed.

In Table 4, it is observed that Bofe clay, despite exhibiting high cadmium removal (91.9%), only removed 33.9%

Table 4 Removal percentage (% R) and amount of metal adsorbed (q) by Brazilian clays

Adsorbent/metal		Ni^{2+}	Cd^{2+}	Zn^{2+}	Cu^{2+}
Bofe	Removal (%)	67.0 ± 0.4	91.9 ± 1.7	33.9 ± 1.1	72.0 ± 2.5
	q (mmol/g)	0.083 ± 0.001	0.116 ± 0.004	0.038 ± 0.003	0.085 ± 0.006
Verde-lodo	Removal (%)	65.4 ± 0.3	94.2 ± 0.0	25.8 ± 0.9	68.4 ± 1.1
	q (mmol/g)	0.081 ± 0.001	0.119 ± 0.000	0.029 ± 0.002	0.080 ± 0.003
Fluidgel	Removal (%)	45.4 ± 2.8	90.5 ± 0.9	93.7 ± 0.4	95.0 ± 0.6
	q (mmol/g)	0.056 ± 0.007	0.115 ± 0.002	0.105 ± 0.001	0.112 ± 0.002
Vermiculite	Removal (%)	86.2 ± 0.5	95.3 ± 0.3	85.9 ± 0.2	83.7 ± 1.1
	q (mmol/g)	0.107 ± 0.002	0.121 ± 0.001	0.096 ± 0.001	0.098 ± 0.003

of Zn^{2+}. Similar behavior was observed in the Verde-Lodo clay, which removed only 25.8% of Zn^{2+}, despite achieving satisfactory removal values for other metals. Fluidgel clay achieved removal rates above 90% for Cd^{2+}, Zn^{2+}, and Cu^{2+}, but only 45.4% for Ni^{2+}. Expanded vermiculite clay presented better performance in removing metal ions. Vermiculite achieved satisfactory removal rates (above 80%) for all metals evaluated, with Ni^{2+} (86.2%) and Cd^{2+} (95.3%) showing the highest removal rates among all clays.

During the experiments, it was observed that the pH of some systems varied constantly, while for others, it remained nearly constant. Tests to evaluate pH change during adsorption experiments were performed. Figure 1 presents pH monitoring data. Solutions that had a pH above the value at which precipitation occurs (indicated by a line) had their pH reduced by an acidic solution (HNO_3, 0.1 mol/L). Tests with Bofe and Verde-lodo clays kept the pH closer to the standard of 4.5, which favored the adsorption process without interfering with the pH. The Fluidgel and vermiculite clays significantly altered the pH of the solution, often bringing it above the minimum precipitation pH.

The sharp increase in pH observed during the experiments with Fluidgel and expanded vermiculite can be attributed to the presence of hydroxides in the clay composition, including alkaline earth metal hydroxides, and to the proton adsorption process (capture of H^+ due to the predominance of charges negative on the clay surface within the pH range in which the experiments were carried out (Neves et al. 2022)). In vermiculite, the octahedral layers contain hydroxides such as $Al(OH)_3$ and $Mg(OH)_2$ (Freitas et al. 2017), which can release hydroxide ions (OH^-) when reacting with water. Furthermore, under low pH conditions, vermiculite allows proton diffusion and subsequent protonation of silanol and aluminol groups, resulting in an increase in pH (Panuccio et al. 2009). It is important to mention that, after each pH measurement, the pH was adjusted to values below 4.5. Also, at the end of the experiment, the pH was adjusted; thus, any potential precipitated material could return to its soluble form. In this way, all the metal present in the liquid medium could be counted as a non-adsorbed solute; i.e., the observed metal reduction occurred only due to adsorption by the surface of the clays.

Therefore, the cadmium with vermiculite system was selected to continue the study, as the removal achieved was the highest in the adsorptive affinity study, and the pH of the solution remained below the minimum for ion precipitation throughout the process. Cadmium ions occur as bivalent ionic species up to a pH of 8.2, a factor that allows satisfactory pH control, even with the use of sodified vermiculite (a fact observed in the subsequent stages of this work). Also, ideally, a good adsorbent should have affinity for the widest range of pollutants possible, as seen with expanded vermiculite.

In the previous work, Neves et al. (2022) carried out the kinetic study of Cd^{2+} adsorption on EV and VNa clays. The investigation concluded that the pseudo-second-order model best described the kinetic data, which is related to the chemisorption of the metal on the solid surface, consistent with the observed ion exchange. The evaluation of kinetic models indicated that mass transfer resistance in external film may be the step that controls the adsorption of Cd^{2+}. In kinetic tests, removal efficiencies greater than 99% were achieved. The characterization analyses indicated possible sites where adsorption/ion exchange occurs, with Si–O–R being a likely site of interaction with the adsorbate (considering R metals such as Mg, Al, Fe, and Si). Other important considerations regarding the previous work are distributed throughout the present text.

Equilibrium study—adsorption isotherms

Figure 2 shows the monocomponent adsorptive equilibrium isotherms of cadmium on expanded (a) and sodified (b) vermiculite at temperatures of 25, 35, and 45 °C. The cadmium adsorption isotherms on expanded vermiculite, Fig. 2a, show a similar favorable behavior at the three temperatures. Figure 2b shows that the cadmium adsorption isotherms on sodified vermiculite (VNa) can be classified as extremely favorable. However, there is a considerable change in the profile of the 45 °C isotherm to the others. This plateau must be explained by physical–chemical changes in the system, which increase chemical interactions at higher temperatures, resulting in an increase in adsorption and ion exchange capacity.

The greater capacity at higher temperatures indicates that the process is endothermic for both the adsorption of Cd^{2+} on EV and VNa clays. In endothermic processes, when the metal is captured by the surface of the solid, energy is absorbed in the form of heat from its surroundings; therefore, the process is favored as the temperature increases (Tran et al. 2016). EV and VNa clays have a negative surface charge within the pH range used in the experiments (Neves et al. 2022), and with an increase in temperature, solubilization of the clay constituents and/or the release of ions into the solution may occur, resulting in an increase in negative charges on the solid surface. This leads to the generation of more active adsorption sites at 45 °C. Regarding ion exchange, the exchangeable ions are Mg^{2+} and Na^+ for EV (CEC, 1.0216 mmol/g) and VNa (CEC, 2.2711 mmol/g), respectively (Neves et al. 2022). Likewise, increasing temperature can favor the release of these cations and the adsorption of Cd^{2+} by clay through ion exchange.

Tables 5 and 6 show the parameters obtained from the model adjustments. The R^2, RMD (%), and *AICc* were used to evaluate the adequacy of the models to the experimental results. The first line of the table contains the value of the

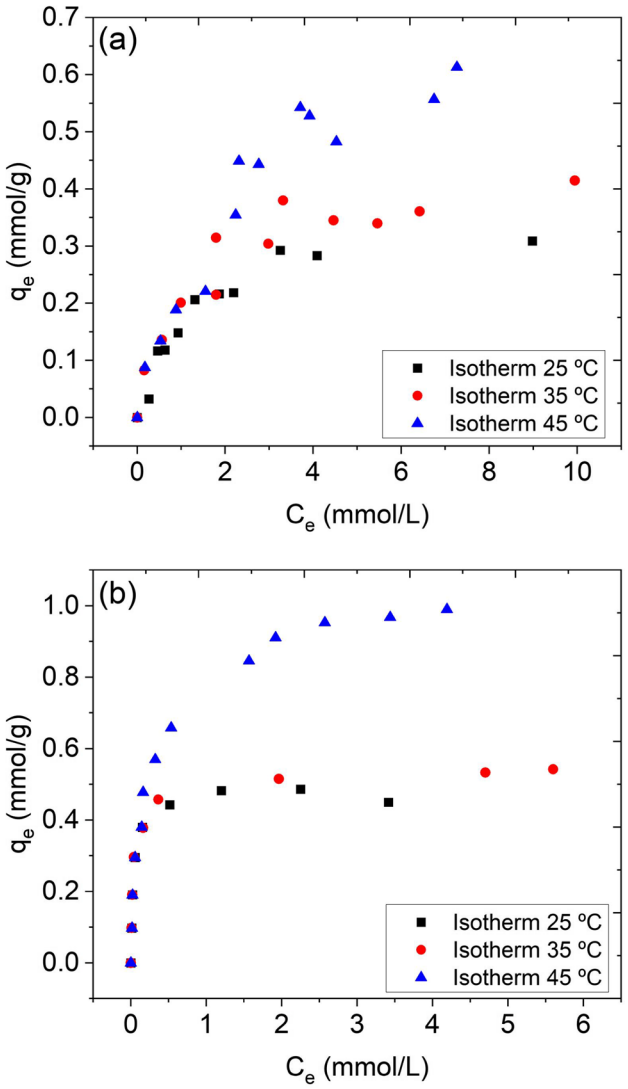

Fig. 2 Cadmium adsorption isotherms on expanded vermiculite (**a**) and sodified vermiculite (**b**) adsorbents at temperatures of 25, 35, and 45 °C

Table 5 Parameters obtained from adjustments of the single-component equilibrium models of expanded vermiculite for different temperatures (25, 35, and 45 °C)

Models	Parameters	Temperatures		
		25 °C	35°C	45 °C
Experimental	q_{max} (mmol/g)	0.295	0.372	0.551
Langmuir	q_{max} (mmol/g)	0.368	0.441	0.834
	K_L (L/mmol)	0.796	0.874	0.371
	R_L	0.123	0.103	0.271
	R^2	0.972	0.946	0.957
	RMD (%)	14.10	9.90	11.51
	AICc	−79.07	−74.02	−72.59
Freundlich	K_F	0.159	0.207	0.242
	n	2.748	3.069	2.040
	R^2	0.901	0.922	0.932
	RMD (%)	26.18	12.13	14.14
	AICc	−64.99	−69.54	−66.74
Redlich-Peterson	K_{RP}	0.241	0.452	0.222
	α_{RP}	0.490	1.175	0.089
	β_{RP}	1.139	0.939	1.503
	R^2	0.976	0.947	0.962
	RMD (%)	12.23	9.49	12.37
	AICc	−75.57	−69.47	−69.99
Dubinin-Radushkevich	q_m (mmol/g)	0.287	0.367	0.584
	β (mol^2/J^2)	$1.6.10^{-7}$	$1.7.10^{-7}$	$3.7.10^{-7}$
	E (KJ/mol)	1.779	1.691	1.169
	R^2	0.782	0.834	0.890
	RMD (%)	10.99	18.31	24.92
	AICc	−64.40	−58.59	−57.50

maximum adsorption capacity (q_{max}), calculated from the average of the last three experimental points. The fits of the Langmuir, Freundlich, Redlich-Peterson, and Dubinin-Radushkevich models for each of the isotherms are presented together in Fig. 3.

From Table 5, it is possible to observe that the Langmuir and Redlich-Peterson models presented a satisfactory adjust to the experimental data of the Cd^{2+} isotherms with EV. Regarding the Cd^{2+} isotherms with VNa, in Table 6, similar behavior was observed. In both systems, the Langmuir and Redlich-Peterson models exhibited the most appropriate fits to the experimental data with highest R^2 and lowest RMD (%) and *AICc* values among models. Comparing the Langmuir and Redlich-Peterson models, it is noted that in the system with EV, the R^2 and RMD (%) values are similar, but the *AICc* for Langmuir is lower. In the system with VNA, the model evaluation parameters indicated that the Langmuir and Redlich-Peterson models were the most suitable, with very close values of R^2, RMD (%), and *AICc*. Both models exhibit a certain degree of similarity, but the Redlich-Peterson model includes empirical coefficients that enhance the fit to the data. On the other hand, the Langmuir model holds significant theoretical significance and finds broader application in adsorption processes. Therefore, hypotheses such as homogeneous surface, monolayer adsorption, and the number of energetically equivalent finite sites are relatively valid due to the satisfactory fit of the Langmuir model.

The q_{max} values of the Langmuir model were close to those obtained experimentally, increasing with increasing temperature, as did the q_m values of the Dubinin-Radushkevich model, a fact that confirms that adsorption is favored with increasing temperature in two systems. The separation factor (R_L) found from the Langmuir model was between 0 and 1 in all cases, indicating that the isotherms are favorable and validating the observed profile of the curves. The value obtained from the model for isotherms with VNa was much

Table 6 Parameters obtained from adjustments of the single-component equilibrium models of sodified vermiculite for different temperatures (25, 35, and 45 °C)

Models	Parameters	Temperatures		
		25 °C	35°C	45 °C
Experimental	q_{max} (mmol/g)	0.473	0.530	0.970
Langmuir	q_{max} (mmol/g)	0.480	0.523	1.001
	K_L (L/mmol)	26.66	27.25	4.900
	R_L	0.0109	0.0065	0.0464
	R^2	0.996	0.988	0.982
	RMD (%)	5.28	5.08	11.02
	AICc	−63.24	−56.55	−69.93
Freundlich	K_F	0.427	0.439	0.711
	n	5.950	6.246	3.521
	R^2	0.887	0.916	0.972
	RMD (%)	21.71	21.41	17.32
	AICc	−38.79	−39.45	−63.93
Redlich-Peterson	K_{RP}	12.201	18.343	10.033
	α_{RP}	25.303	36.446	12.032
	β_{RP}	1.0113	0.9551	0.8464
	R^2	0.962	0.995	0.995
	RMD (%)	5.22	4.40	5.76
	AICc	−56.40	−58.48	−82.23
Dubinin-Radushkevich	q_m (mmol/g)	0.482	0.526	0.923
	β (mol^2/J^2)	$1.1.10^{-8}$	$1.0.10^{-8}$	$2.4.10^{-8}$
	E (KJ/mol)	6.807	7.051	4.518
	R^2	0.978	0.984	0.952
	RMD (%)	7.24	5.61	16.27
	AICc	−48.66	−48.93	−53.52

closer to 0, suggesting that these isotherms are even more favorable than those with EV (McCabe et al. 2000).

The Freundlich model exhibited a low R^2 value and higher RMD (%) and *AICc* among the models, indicating a non-predictive fit to the data. However, despite the lack of prediction, fluctuations in observed parameter values hold physical significance in the studied system. The Freundlich constant K is associated to the adsorption capacity. In equilibrium tests with VNa, an increase of K value was observed with increasing temperature, consistent with the increase in maximum capacity observed experimentally. The constant n is indicative of the heterogeneity of adsorption sites, and its value remains relatively close for the three isotherms, as expected given the use of the same adsorbent material. Nonetheless, following sodium treatment, this parameter increased, suggesting a heterogeneity of active sites. In the sodification treatment, leaching and formation of ion exchange sites take place. In other words, in the final clay, there are adsorption sites from the clay itself as well as sites created during leaching that have been occupied by sodium, which exhibit distinct energies.

When comparing the model fittings to the two systems, it is observed that the system with VNa exhibited lower RMD (%) and *AICc* values and higher R^2 values. This suggests that the lower complexity of the adsorbent matrix facilitated a better fit of the models to the experimental data. At 25°C, the Langmuir model provided the best fit to the experimental data, with the maximum cadmium adsorption capacity on expanded vermiculite being 0.368 mmolCd/g (41.37 mgCd/g) and on sodium-modified vermiculite being 0.480 mmolCd/g (53.93 mgCd/g). A positive effect of sodium treatment on the adsorptive capacity is observed, with sodium-modified clay showing a 30.37% increase in adsorptive capacity. At 45°C, the VNa clay achieved the highest experimental removal capacity 0.970 mmolCd/g (112.55 mgCd/g), more than doubling the value obtained at 25°C.

The q_{max} value reported by da Fonseca et al. (2006) was 56.2 mgCd/g for Cd^{2+} adsorption on vermiculite at room temperature (25 °C). Considering the structural and chemical differences between the different batches of this natural adsorbent, the q_{max} obtained in this work was close. Abollino et al. (2008) obtained cadmium adsorptive capacity of 37.61 mg/g in a fixed bed of vermiculite and 5.20 mg/g on montmorillonite. Panuccio et al. (2009) carried out the study of cadmium adsorption on three different minerals, where the order of greatest adsorption capacity obtained was vermiculite > zeolite > pumice. These factors indicate the high viability of vermiculite in removing cadmium among other minerals. The maximum adsorption capacity of cadmium on vermiculite was 16.07 mg/g. The cited works and other results from the literature on cadmium adsorption on other conventional and non-conventional adsorbents are presented in Table 2S-1 (see Sect. 2S of the Supplementary Material). The vermiculite clays used in this study showed very satisfactory removal capacity, considerably superior to other clay minerals commonly reported in the literature, such as montmorillonite and kaolinite.

The simplified adsorption batch design is presented in the Supplementary Material (see Sect. 3S, Fig. 3S-1). This approach is used to determine the required amount of adsorbent to remove Cd^{2+} from an effluent at a fixed concentration and temperature, considering different efficiency values. The results highlighted the superiority of VNa clay over EV in removing Cd^{2+}. The amount of VNa required is much lower than that of EV under the same conditions. For example, to remove 90% of Cd^{2+} from 10 L of solution, up to 12.7 times more EV are required compared to VNa. This demonstrates that the sodified adsorbent is much more efficient in adsorbing Cd^{2+} ions.

Affinity tests (Table 4) indicated that EV clay was able to remove 95.3% of the Cd^{2+} present in the solution. Equilibrium experiments demonstrated that adsorption is extremely favorable, with satisfactory removal results at different temperatures. The regeneration and reuse of the adsorbent

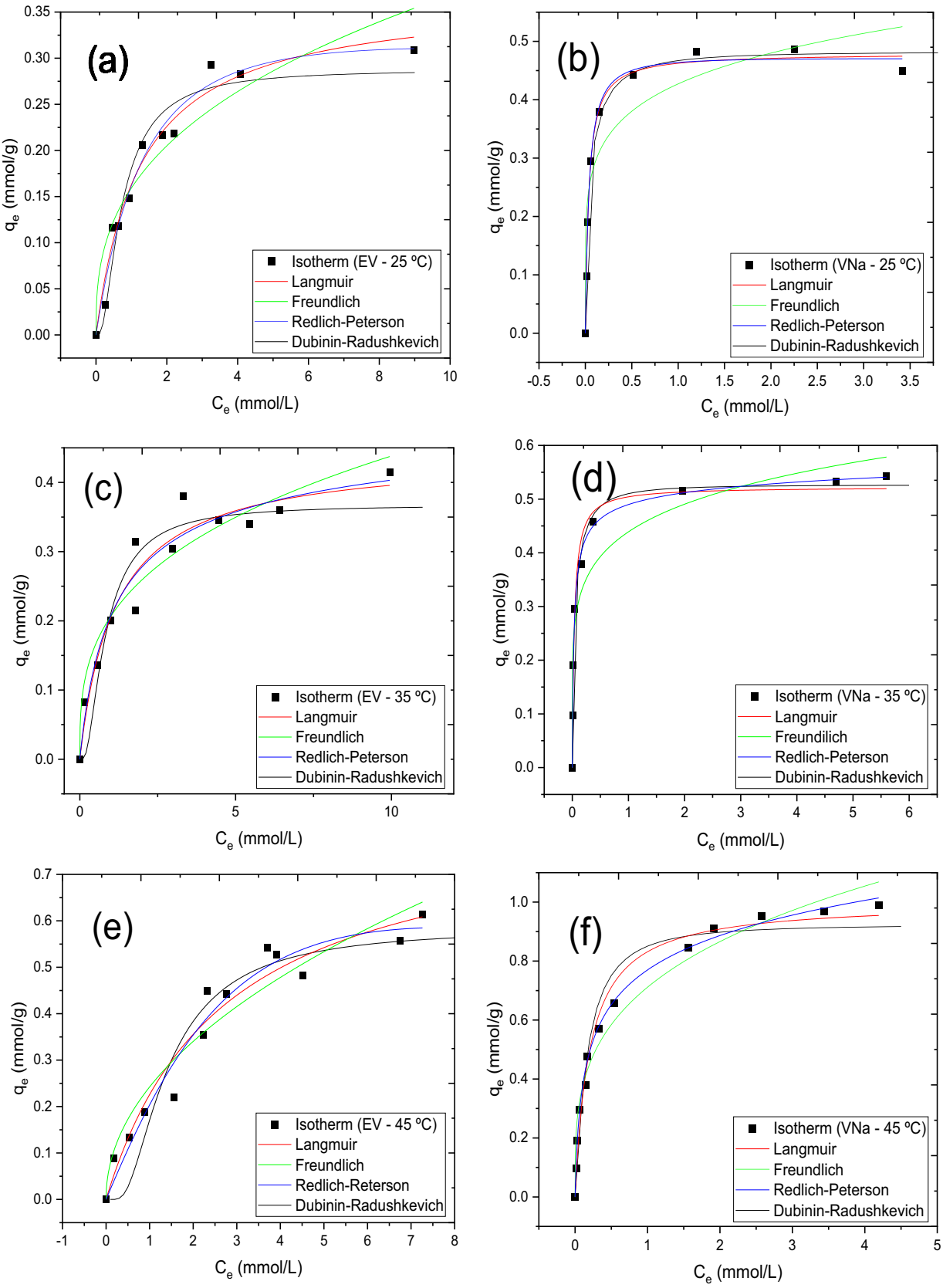

Fig. 3 Adjustments of the Langmuir, Freudlich, Redlich-Peterson, and Dubinin-Radushkevich single-component equilibrium models for isotherms with EV at 25 °C (**a**), VNa at 25 °C (**b**), EV at 35 °C (**c**), VNa at 35 °C (**d**), EV at 45°C (**e**), and VNa at 45 °C (**f**)

have already been studied in previous works (de Brião et al. 2020, 2021), which evaluated the reuse of expanded vermiculite in five adsorption/desorption cycles. Brião et al. (2020) used Brazilian expanded vermiculite in batch experiments for neodymium adsorption. It was observed that the metal adsorption efficiencies in the cycles were greater than 94% in all experiments, and the desorption capacity reached 95% in the 5th cycle, using $CaCl_2$ (0.3 mol/L) as eluent. The same group subsequently evaluated the performance of expanded vermiculite in removing dysprosium (Brião et al. 2021) and observed high adsorption and desorption efficiencies in the five cycles evaluated. Removal efficiencies above 99% were achieved in all cycles, with desorption capacities above 94% during the experiments, using $Mg(NO_3)_2$ (0.2 mol/L) as eluent. Both studies used a metal concentration of 1 mmol/L, the same concentration used in the affinity adsorption experiments in the present work, and demonstrated that the clay can be recovered and reused without damaging the adsorbent solid after five cycles.

Thermodynamic study

The thermodynamic quantities evaluated were changes in enthalpy (ΔH), entropy (ΔS), and Gibbs energy (ΔG), obtained from linear fits of the graph of $\ln(K)$ versus $1/T$, where K is the equilibrium constant appropriate to the system. The equilibrium constant (K) can vary depending on which equilibrium model best represents the system and best fits the Van't Hoff equation (Table 2). In this case, the K value was the linear coefficient of the region of infinite dilution of the isotherms, obtained from Henry's law (Table 2).

Figure 4S-1 (see Sect. 4S in Supplementary Material) shows the graphs of the fit of the Van't Hoff equation to $\ln(K)$ versus $1/T$ data for cadmium adsorption systems on EV and VNa. A linear trend was observed for both systems, which indicates that Henry's Law represented the equilibrium constant well. Table 7 shows the ΔH, ΔS, and ΔG values for the systems with EV and VNa, respectively. The R^2 of the linear regression was used to assess the applicability of the method for obtaining the thermodynamic quantities of the system.

Table 7 Thermodynamic quantities obtained from Henry's law applied to Cd^{2+} adsorption isotherms on expanded vermiculite and sodium-modified vermiculite

	Expanded vermiculite			
T (°C)	ΔG (KJ/mol)	ΔH (kJ/mol)	ΔS (J/(mol·K)	R^2
25	−1.264	13.259	48.958	0.811
35	−1.989			
45	−2.232			
	Sodified vermiculite			
T (°C)	ΔG (KJ/mol)	ΔH (kJ/mol)	ΔS (J/(mol·K)	R^2
25	−5.817	41.886	159.522	0.928
35	−6.967			
45	−9.027			

From Table 7, for all cases, the ΔG values are negative, indicating the spontaneity of the process and its thermodynamic feasibility. The Gibbs energy change value can predict the nature of the bonds formed during adsorption (Yu et al. 2001), where the range from 0 to − 20 kJ/mol corresponds to physisorption, and when the values are between − 80 and − 400 kJ/mol, chemisorption occurs. Both in the case of Cd^{2+} adsorption on expanded vermiculite and sodium-modified vermiculite, the ΔG values are within the physisorption range, corroborating the indication provided by the sorption free energy (E) of the Dubinin-Radushkevich model.

The entropy change values (ΔS) of adsorption with EV and VNa were + 48.96 and + 159.52 kJ/(mol·K), respectively. Positive values indicate that the entropy of the system increases after adsorption, where the adsorbate exhibits high affinity and the disorder at the solid/fluid interface increases, potentially leading to structural alterations in the adsorbent.

The ΔH values were also positive (endothermic character) within the studied range, indicating that the sorption process of Cd^{2+} is favored by the increase in temperature. These values also indicate the nature of the process (Saha and Chowdhury 2011), where the system with EV falls within the range characterized as physisorption (2.1 to 20.9 kJ/mol) and the system with VNa falls between the physisorption and chemisorption range (80 to 200 kJ/mol).

Studies reported in the literature have investigated the adsorption of Cd^{2+} ions on both conventional and unconventional adsorbents. Fan et al. (2008) conducted thermodynamic studies on the biosorption of Cd^{2+} using biomass from the bacterium *Penicillium simplicissimum* and obtained a relatively similar ΔH value (20.03 kJ/mol) to that found in this work, together with a positive value of ΔS. However, these observations depend on the physicochemical characteristics of the adsorbent used, as revealed in Table 4S-1 (See Sect. 4S of the Supplementary Material), which presents the values of ΔH, ΔG, and ΔS for different adsorbents.

Evaluation of ion-exchange equilibrium

During the equilibrium experiments, the concentrations of relevant light metals released by the clay mineral were also measured to apply models that describe the profile more adequately. The binary Langmuir model was a good fit for the ion exchange system of Cd^{2+} with Mg^{2+} on expanded vermiculite. The choice of Mg^{2+} for assessing the ion-exchange equilibrium is due to the fact that magnesium is part of the clay constitution, and a previous study (Neves et al. 2022) with the same clay indicated that in expanded vermiculite the exchangeable Mg^{2+} are 97.1%

(A) Expanded Vermiculite (ion exchange between Cd^{2+} and Mg^{2+}) - binary Langmuir model.

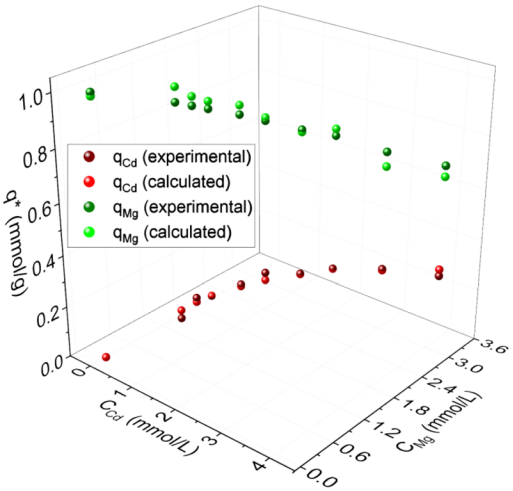

(**B**) Sodified Vermiculite (ion exchange between Cd^{2+} and Na^{+}) - binary Langmuir-Freundlich model

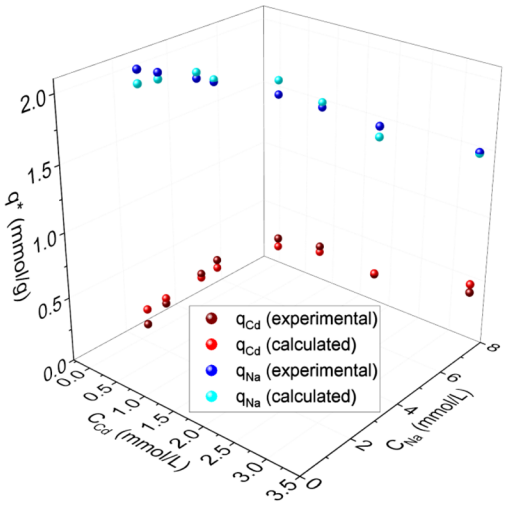

Fig. 4 Fittings of the binary Langmuir model to the ion exchange of Cd^{2+} ions with Mg^{2+} on expanded vermiculite (**A**) and of the binary Langmuir–Freundlich model to the ion exchange of Cd^{2+} ions with Na^{+} in sodified vermiculite (**B**), at 25 °C and pH 6

of all ions available for ion exchange (calculated from the data reported in (Neves et al. 2022)). Figure 4 shows the experimental and model-calculated profile of this system at 25 °C. The isotherms at 35 and 45 °C are presented in Sect. 5S (Figs. 5S-A, B, C and D) of the Supplementary Material (Sect. 5S).

The binary Langmuir model presented a satisfactory fit for the ion exchange system of Cd^{2+} with Mg^{2+} on expanded vermiculite. The ion exchange isotherms of this system exhibited the theoretically expected profile. At higher concentrations of Cd^{2+}, a greater amount of Mg^{2+} is released into the solution, and the amount of heavy metal absorbed by vermiculite is very close to the amount of light metal released; that is, a satisfactory stoichiometric proportion is observed.

The fit parameters of the binary Langmuir model to the experimental data of isotherms with EV (25, 35, and 45°C) are presented in Table 8. For this adjustment, the value of $q_{Mg(max)}$ was set at 1.022 mmol/g, which is the maximum value of exchangeable Mg^{2+} obtained in the CEC experiment (Neves et al. 2022). The model fitted the experimental data relatively well, as all R^2 values approached 0.9 with lower RMD (%) for the adjustment of magnesium data. The *AICc* values were relatively close for all temperatures, with slightly lower values at 25°C indicating better model prediction at this temperature. According to the coefficients of determination, there was no significant reduction, indicating that the four adjusted parameters of this model have a good ability to predict the ion exchange equilibrium (Montgomery et al. 2012).

Table 8 Adjusted parameters of the binary Langmuir model to experimental equilibrium data for the ion exchange of Cd^{2+} with Mg^{2+} on expanded vermiculite, and binary Langmuir–Freundlich model for the ion exchange of Cd^{2+} ions with Na^{+} on sodified vermiculite

Parameters	Equilibrium temperature		
	25 °C	35 °C	45 °C
	Expanded Vermiculite—binary Langmuir model		
$q_{Cd(max)}$ (mmol/g)	0.893	0.954	0.8515
$q_{Mg(max)}$ (mmol/g)	1.022	1.022	1.022
$K_{l,Cd}$ (L/mmol)	76.022	159.878	1119.755
$K_{l,Mg}$ (L/mmol)	187.623	377.051	656.669
F_{obj}	0.015	0.046	0.081
R^2	0.965	0.897	0.885
RMD_{Cd} (%)	14.89	16.67	26.50
RMD_{Mg} (%)	3.87	5.35	7.29
$AICc_{Cd}$	−56.03	−43.42	−36.55
$AICc_{Mg}$	−42.01	−44.49	−43.83
	Sodified vermiculite—binary Langmuir–Freundlich model		
$q_{Cd(max)}$	1.542	1.522	1.285
$q_{Na(max)}$	2.271	2.271	2.271
$K_{l,Cd}$	39,759.6	40,474.7	276.6
$K_{l,Na}$	65,219.5	64,080.9	95.16
K_{Cd}	0.25	0.25	0.25
K_{Na}	0.25	0.25	0.67
F_{obj}	0.068	0.225	0.073
R^2	0.873	0.867	0.988
RMD_{Cd} (%)	23.99	24.94	68.03
RMD_{Na} (%)	13.92	6.05	61.71
$AICc_{Cd}$	75.44	15.96	7.50
$AICc_{Na}$	121.05	29.83	21.97

Regarding the ion exchange between magnesium and cadmium on the EV, the $q_{Cd(max)}$ values did not agree with the adsorptive modeling. Langmuir q_{max} values indicated 0.368 mmol/g at 25 °C, 0.441 mmol/g at 35 °C, and 0.834 mmol/g at 45 °C (Table 5). It is noted that only at 45 °C was the $q_{Cd(max)}$ value close to the Langmuir q_{max} value. The constant of binary-Langmuir equilibrium indicated that at temperatures of 25 and 35°C, the exchanger exhibits greater selectivity for Mg^{2+}, because the values of $K_{L,Mg}$ were higher than $K_{L,Cd}$. The opposite occurs at 45°C. Additionally, the increase in K_L values with increasing temperature reveals that adsorbent-adsorbate interactions are increasing, that is, becoming stronger, which may be related to the increased dominance of chemisorption or ion exchange mechanisms (Costa et al. 2018). The R^2 values indicate that the quality of fit decreases with increasing temperature and the RMD (%) and *AICc* values indicate that the model is more suitable for magnesium (lower values). It is important to note that in EV, magnesium ions are the most exchangeable in the ion exchange mechanism; however, other removal processes are related to the uptake of Cd^{2+} from the liquid medium, such as adsorption. The decrease in R^2 of the model used to represent ion exchange in EV can indicate that other mechanisms are present. Figure 4 shows that the model adjustments of the binary Langmuir model provided parameters capable of predicting the experimental data; however, the physical meaning of these parameters was not observed, since the calculated values of q_{max} were far from those observed experimentally.

In VNa, the Na^{+} ion represents 97.8% of the total ions available for ion exchange (Neves et al. 2022). The binary Langmuir model was used to evaluate ion exchange of cadmium and sodium ions; however, the results were not satisfactory. The profile differed greatly from the theoretically expected, as the adsorption of Cd^{2+} and the desorption of Na^{+} did not exhibit a stoichiometric relationship. Additionally, the behavior of the Na^{+} desorption and Cd^{2+} adsorption profiles were different, since the sodium desorption isotherm was close to linear and the cadmium adsorption profile was extremely favorable. This is because ion exchange is not the only removal mechanism in this system; adsorption may also occur through electrostatic attractions or complexation by silanol and aluminiol groups (Badawy et al. 2010).

Therefore, the addition of empirical exponential coefficients to the concentrations in the liquid phase was proposed using the binary Langmuir–Freundlich model. Figure 4 and Table 8 also present the adjustments and parameters obtained with the binary Langmuir–Freundlich model. The isotherms at 35 and 45 °C are presented in Sect. 5S in the Supplementary Material.

For sodified vermiculite (Freundlich-Langmuir binary model), the $q_{Na(max)}$ value was set at 2.271 mmol/g, which is the maximum exchangeable Na^{+} value obtained in the CEC experiment (Neves et al. 2022). Among the coefficients of determination (R^2), the one obtained at 45°C was the highest (0.988), and the *AICc* was the lowest, for both Na^{+} and Cd^{2+}, indicating that the model is more adequate at 45°C. At 25°C and 35°C, the correlation coefficients did not indicate a good fit; R^2 were lower, and *AICc* values were higher. The RMD (%) of the system with EV was lower than that with VNA clay, and comparing the deviation of metals, the RMD (%) was lower for sodium, released during ion exchange. It is important to highlight that at 25°C and 35°C, the values of the q_{max} parameter calculated by the model are far from those obtained experimentally, whereas at 45°C the best approximation of the calculated value to the experimental value is observed. The large number of parameters in this model significantly reduced its representativeness, especially for the 25 and 35 °C isotherms. Comparing with single-component models of Cd^{2+} adsorption, the binary Langmuir–Freundlich model appeared to be much less suitable, except for the 45°C isotherm. This is due to the difference

in the shape of the Cd^{2+} adsorption and Na^{+} desorption isotherms, representing a significant discrepancy in the principle of electroneutrality of ion exchange.

From Fig. 4, for both systems the models were predictive, as the profiles provided by the models are very close to the experimental ones. Figure 5S (Supplementary Material) demonstrates the same tendency of proximity between calculated values and experimental values for all temperatures. However, the values of the q_{max} parameters were far from the experimental ones. That is, in general, the models were predictive, but the parameters provided do not represent the experimental q_{max} capacities values.

In summary, both models quantitatively represented the equilibrium of the two systems well, as can be seen in Fig. 4, but few parameters provided relevant information for qualitative analysis; that is, the parameters obtained do not present a physical representation of what happens in the systems evaluated. This is possibly due to the complexity of the matrix used in adsorption, which exhibits high heterogeneity in the types of sites, and the different uptake systems involved, adsorption and ion exchange together.

The single-component models proved to be more descriptive, allowing the observation of the endothermic behavior of the system. In effluent treatment applications, knowledge of parameters such as temperature, particle size, and adsorbent dosage provided by this type of modeling is important. However, these analyses are less costly and faster, besides the fact that the light metals released by clay minerals do not affect the final toxicity of the treated effluent.

Characterizations

Helium gas picnometry and mercury porosimetry are important analyses of the physical structure of the adsorbent, aimed to determine the real and apparent densities, respectively. Table 9 presents the real and apparent densities, as well as the adsorbent porosities (calculated by Eq. 22) before and after the adsorption process.

Evaluating the real density values of the samples, an increase in the adsorbent density is observed after the sodification process (modification process from EV to VNa). Also, after the adsorption of Cd^{2+}, both in EV and in VNa, there was an increase in density. This behavior is attributed to the contraction of the lamella during water absorption, both in the sodification process and in the liquid-phase adsorption process.

Table 9 Densities and porosities obtained from the adsorbents before and after contamination, obtained by mercury porosimetry and helium gas pycnometry techniques

	EV	EV + Cd	VNa	VNa + Cd
Real density (g/cm^3)	2.23	2.59	2.66	2.70
Apparent density (g/cm^3)	0.640	0.516	1.071	0.935
Porosity (%)	28.67	19.92	40.31	34.69

The increase in density after adsorption on clays was accompanied by a decrease in solid porosity. The reduction in the adsorbent porosity after contamination with Cd^{2+} occurs due to the contraction of the solid and the pore filling with the adsorbent. It is important to note that after sodium treatment, there was an increase in porosity, possibly due to the low pH applied in this methodology, which leached some of the exchangeable interlamellar ions.

The results of thermogravimetric and differential thermal analyses are presented in Fig. 5, for expanded and sodified vermiculite, pre- and post-adsorption. In the thermograms (Fig. 5), the thermogravimetric curve (TG), indicated by the black line, depicts a decrease in mass as a function of temperature. Both curves exhibit similar behavior, except for sodified vermiculite, which showed better thermal stability without a sharp mass drop at high temperatures. The sharp drops can be more clearly observed through the derivative of this curve (DTG). In the DTG curves, indicated by the red line, there is a peak in the temperature range of 73 to 106 °C, corresponding to the loss of water adsorbed in its structure and decomposition of microorganisms. Another loss occurs between 180 and 220 °C, related to dehydroxylation (Nishikawa et al. 2012).

The differential thermal analysis (DTA), indicated by the blue line, showed that all the changes that occurred are endothermic, with peaks close to those of the DTG curve. Peaks between 863 and 901 °C were observed in three of the samples, exhibiting endothermic behavior, which may represent the melting of the adsorbent (Souza Santos 1975). This peak is not observed for sodified vermiculite, corroborating the fact that sodium treatment improves the thermal stability of the adsorbent.

Additional characterization analyses of EV and VNa are available in the study by Neves et al. (2022). In this work, the kinetics of cadmium adsorption and ion exchange on EV and VNa were evaluated, as well as the CEC, and complementary characterizations (XRD, SEM, EDS, and FTIR). The characterization results presented in the present work agree with other analyses carried out previously and with the adsorption and ion exchange process that took place.

The increase in density observed (Table 9) after the sodification and Cd^{2+} adsorption steps was expected, as the scanning electron microscopy (SEM) images of the material indicated the contraction of clay lamellae after processes involving water absorption. Furthermore, the surface areas of the particles decreased after sodification and contamination: EV, 26.5 m^2/g; EV-Cd, 9.9 m^2/g; VNa, 11.1 m^2/g; and VNa-Cd, 6.7 m^2/g (Neves et al. 2022). The reduction in surface area also hinted at the observed decrease in density.

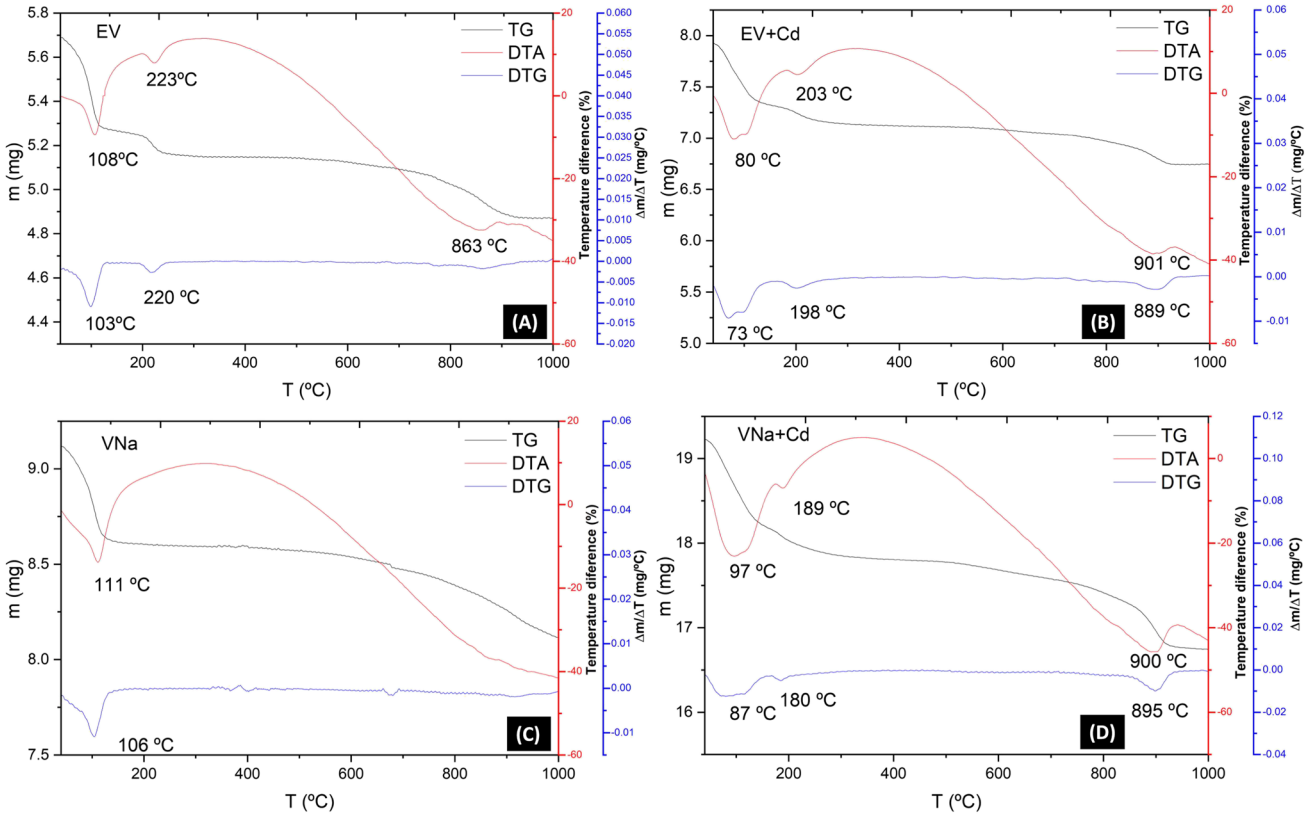

Fig. 5 Thermogravimetric analyses of expanded vermiculite (**A**, **B**) and sodified vermiculite (**C**, **D**) before (**A**, **C**) and after (**B**, **D**) the Cd^{2+} adsorption process

Despite the lamellae contraction, there was an increase in porosity during the modification from EV to VNa, which, as mentioned previously, can be attributed to the leaching of constituent ions and the lamellae spacing. This was observed in energy-dispersive X-ray spectroscopy (EDS) analyses, where the percentages of original constituents decreased while sodium increased significantly.

The characterization analyses corroborated the analyses previously reported and evidenced the improvement promoted in the solid's characteristics after the sodification process. Vermiculite clay showed promise in capturing Cd^{2+} from aqueous media, with sodified clay demonstrating the best adsorptive performance.

Conclusions and perspectives

In this study, among the Brazilian clays evaluated (Bofe, Verde-lodo, commercial Fluidgel, and expanded vermiculite), expanded vermiculite exhibited superior performance in removing toxic metals. Following modification through sodification, its efficiency was significantly enhanced. Affinity tests indicated that the adsorptive system between expanded vermiculite and cadmium yielded the most promising results, serving as a model to evaluate the ion exchange between the pollutant and exchangeable ions within the solid. At 25 °C, expanded vermiculite demonstrated a maximum adsorption capacity of 0.368 mmol/g (41.37 mgCd/g), while sodified vermiculite exhibited 0.480 mmol/g (53.93 mgCd/g). The observed improvement highlighted the importance of the sodification process for Cd^{2+} uptake. The process was found to be spontaneous and endothermic.

Single-component models proved to be effective in predicting adsorption behavior, particularly the Langmuir model, which was used as the basis for binary fits. The binary models were predictive in relation to the experimental values. The binary Langmuir model better represented the ion exchange between Cd^{2+} and Mg^{2+} on expanded vermiculite, whereas the binary Langmuir–Freundlich model better represented the exchange of Cd^{2+} and Na^{+} on sodified vermiculite. The binary model can be used in different systems, such as a fixed bed column, which is an open system and where the removed ion leaves the system completely, thus explaining the increased adsorption capacity observed in fixed beds compared to batch systems. The single-component models proved to be adequate to describe the removal of cadmium from the liquid medium by clays.

The characterization analyses corroborated previous results obtained by our research group (Neves et al. 2022). There was a decrease in density and porosity after liquid phase procedures, due to the contraction of the lamellae and filling of the pores. In summary, the treatment of vermiculite with sodium substantially improved the adsorbent efficiency, showing promise for modifying vermiculite to remove metal contaminants.

As future perspectives of the present study, the stability and recovery of the adsorbent, the selection of eluents, the evaluation of adsorption/desorption cycles, the study of adsorption in dynamic fixed-bed systems, and competitive adsorption in multicomponent systems need to be investigated.

Supplementary Information The online version contains supplementary material available at https://doi.org/10.1007/s11356-024-34496-z.

Acknowledgements The authors thank Brasil Minérios and Dolomil.

Author contribution Conceptualization: Melissa G. A. Vieira, Reginaldo Guirardello, Henrique Santana de Carvalho Neves.

Literature search and data analysis: Henrique Santana de Carvalho Neves, Melissa G. A. Vieira, Reginaldo Guirardello.

Writing—original draft preparation: Henrique Santana de Carvalho Neves, Talles B. da Costa, Thiago L. da Silva.

Writing—review and editing: Talles B. da Costa, Thiago L. da Silva, Melissa G. A. Vieira, Meuris G. C. da Silva, Reginaldo Guirardello.

Supervision: Melissa G. A. Vieira, Reginaldo Guirardello, Meuris Gurgel Carlos da Silva.

Funding This work was supported by the Coordination of Superior Level Staff Improvement (CAPES, Grant # 88887.200617/2018–00), the São Paulo Research Foundation (FAPESP, Grant # 2017/18236–1), and the National Council for Scientific and Technological Development (CNPq, Grants # 310039/2023–1, #152592/2022–9, # 307913/2021–0, and # 308046/2019–6).

Data availability Not applicable.

Code availability Not applicable.

Declarations

Competing interests The authors declare no competing interests.

Ethics approval and consent to participate Not applicable.

Consent for publication Not applicable.

References

Abollino O, Giacomino A, Malandrino M, Mentasti E (2008) Interaction of metal ions with montmorillonite and vermiculite. Appl Clay Sci 38:227–236. https://doi.org/10.1016/j.clay.2007.04.002

Ahmaruzzaman M (2011) Industrial wastes as low-cost potential adsorbents for the treatment of wastewater laden with heavy metals. Adv Colloid Interface Sci 166:36–59. https://doi.org/10.1016/j.cis.2011.04.005

Antonelli R, Malpass GRP, Da Silva MGC, Vieira MGA (2020) Adsorption of ciprofloxacin onto thermally modified bentonite clay: experimental design, characterization, and adsorbent regeneration. J Environ Chem Eng 8:104553. https://doi.org/10.1016/j.jece.2020.104553

Azamfire B, Bulgariu D, Bulgariu L (2020) Efficient removal of toxic mmetal ions (Pb(II) and Hg(II) ions in single component systems by adsorption on Romanian clay material. Rev Chim 71:37–47. https://doi.org/10.37358/RC.20.7.8223

Badawy NA, El-Bayaa AA, Abd AlKhalik E (2010) Vermiculite as an exchanger for copper(II) and Cr(III) ions, kinetic studies. Ionics (kiel) 16:733–739. https://doi.org/10.1007/s11581-010-0456-8

Bassam R, El Hallaoui A, El Alouani M et al (2021) Studies on the removal of cadmium toxic metal ions by natural clays from aqueous solution by adsorption process. J Chem 2021:1–14. https://doi.org/10.1155/2021/7873488

Bonate P, Steimer J-L (2011) Pharmacokinetics pharmacodynamics modeling simulation. Springer, San Antonio, Texas, TX, USA

Cantuaria ML, Nascimento ES, Neto AFA et al (2015) Removal and recovery of silver by dynamic adsorption on bentonite clay using a fixed-bed column system. Adsorpt Sci Technol 33:91–103. https://doi.org/10.1260/0263-6174.33.2.91

Cantuaria ML, De Almeida Neto AF, Nascimento ES, Vieira MGA (2016) Adsorption of silver from aqueous solution onto pretreated bentonite clay: complete batch system evaluation. J Clean Prod 112:1112–1121. https://doi.org/10.1016/j.jclepro.2015.07.021

Costa CSD, da Silva MGC, Vieira MGA (2018) Investigation of the simultaneous biosorption of toxic metals through a mixture design application. J Clean Prod 200:890–899. https://doi.org/10.1016/j.jclepro.2018.07.314

da Fonseca MG, de Oliveira MM, Arakaki LNH (2006) Removal of cadmium, zinc, manganese and chromium cations from aqueous solution by a clay mineral. J Hazard Mater 137:288–292. https://doi.org/10.1016/j.jhazmat.2006.02.001

da Silva TL, da Silva MGC, Vieira MGA (2021) Palladium adsorption on natural polymeric sericin-alginate particles crosslinked by polyethylene glycol diglycidyl ether. J Environ Chem Eng 9:105617. https://doi.org/10.1016/j.jece.2021.105617

de Almeida Neto AF, Vieira MGA, da Silva MGC (2014) Insight of the removal of nickel and copper ions in fixed bed through acid activation and treatment with sodium of clay. Brazilian J Chem Eng 31:1047–1056. https://doi.org/10.1590/0104-6632.20140314s0000197676

de Assis Neto PC, Sales LPB, Oliveira PKS et al (2023) Expanded vermiculite: a short review about its production, characteristics, and effects on the properties of lightweight mortars. Buildings 13:823. https://doi.org/10.3390/buildings13030823

de Brião GV, da Silva MGC, Vieira MGA (2020) Neodymium recovery from aqueous solution through adsorption/desorption onto expanded vermiculite. Appl Clay Sci 198:105825. https://doi.org/10.1016/j.clay.2020.105825

de Brião GV, da Silva MG, Vieira MGA (2021) Expanded vermiculite as an alternative adsorbent for the dysprosium recovery. J Taiwan Inst Chem Eng 127:228–235. https://doi.org/10.1016/j.jtice.2021.08.022

de Brião GV, Lopes CB, Trindade T et al (2024) NdFeB magnet scrap valorization by leaching and recovery of rare earth metals by sorption on low-cost expanded clay. J Ind Eng Chem 131:558–568. https://doi.org/10.1016/j.jiec.2023.10.060

de Farias ABV, da Costa TB, da Silva MGC, Vieira MGA (2022a) Development of novel composite adsorbents based on biopolymers/vermiculite using the ionic imprinting technique for cerium biosorption. J Environ Chem Eng 10:108730. https://doi.org/10.1016/j.jece.2022.108730

de Farias ABV, da Costa TB, da Silva MGC, Vieira MGA (2023) Cerium biosorption onto alginate/vermiculite-based particles functionalized with ionic imprinting: kinetics, equilibrium, thermodynamic, and reuse studies. Int J Biol Macromol 241:124542. https://doi.org/10.1016/j.ijbiomac.2023.124542

de Freitas ED, de Almeida HJ, Vieira MGA (2017) Binary adsorption of zinc and copper on expanded vermiculite using a fixed bed column. Appl Clay Sci 146:503–509. https://doi.org/10.1016/j.clay.2017.07.004

de Freitas ED, de Almeida HJ, de Almeida Neto AF, Vieira MGA (2018) Continuous adsorption of silver and copper by Verdelodo bentonite in a fixed bed flow-through column. J Clean Prod 171:613–621. https://doi.org/10.1016/j.jclepro.2017.10.036

de Neves HS, C, da Silva TL, da Silva MGC, et al (2022) Ion exchange and adsorption of cadmium from aqueous media in sodium-modified expanded vermiculite. Environ Sci Pollut Res 29:79903–79919. https://doi.org/10.1007/s11356-021-16841-8

Dubinin MM, Radushkevich LV (1947) Equation of the characteristic curve of activated charcoal. Proc Acad Sci USSR, Phys Chem Sect 55:331–333

Essebaai H, Lgaz H, Alrashdi AA et al (2022) Green and eco-friendly montmorillonite clay for the removal of Cr(III) metal ion from aqueous environment. Int J Environ Sci Technol 19:2443–2454. https://doi.org/10.1007/s13762-021-03303-4

Fan T, Liu Y, Feng B et al (2008) Biosorption of cadmium(II), zinc(II) and lead(II) by Penicillium simplicissimum: Isotherms, kinetics and thermodynamics. J Hazard Mater 160:655–661. https://doi.org/10.1016/j.jhazmat.2008.03.038

de Farias MB, Spaolonzi MP, da Silva TL, et al (2022b) Natural and synthetic clay-based materials applied for the removal of emerging pollutants from aqueous medium. In: Advanced Materials for Sustainable Environmental Remediation. Elsevier, pp 359–392

Febrianto J, Kosasih AN, Sunarso J et al (2009) Equilibrium and kinetic studies in adsorption of heavy metals using biosorbent: a summary of recent studies. J Hazard Mater 162:616–645. https://doi.org/10.1016/j.jhazmat.2008.06.042

Fiyadh SS, AlSaadi MA, Jaafar WZ et al (2019) Review on heavy metal adsorption processes by carbon nanotubes. J Clean Prod 230:783–793. https://doi.org/10.1016/j.jclepro.2019.05.154

Freundlich HMF (1906) Over the adsorption in solution. J Phys Chem 57:385–471

Galindo LSG, de Almeida Neto AF, da Silva MGC, Vieira MGA (2013) Removal of cadmium(II) and lead(II) ions from aqueous phase on sodic bentonite. Mater Res 16:515–527. https://doi.org/10.1590/S1516-14392013005000007

Khan S, Ajmal S, Hussain T, Rahman MU (2023) Clay-based materials for enhanced water treatment: adsorption mechanisms, challenges, and future directions. J Umm Al-Qura Univ Appl Sci. https://doi.org/10.1007/s43994-023-00083-0

Langmuir I (1918) The adsorption of gases on plane surfaces of glass, mica and platinum. J Am Chem Soc 40:1361–1403. https://doi.org/10.1021/ja02242a004

Marcos C, Rodríguez I (2014) Some effects of trivalent chromium exchange of thermo-exfoliated commercial vermiculite. Appl Clay Sci 90:96–100. https://doi.org/10.1016/j.clay.2013.12.032

McCabe WL, Smith JC, Harriott P (2000) Unit operations of chemical engineering, 6th edn. Mc Graw Hill, USA

Montgomery DC, Peck EA, Vining GG (2012) Introduction to linear regression analysis, 5a edn. John Wiley & Sons, New Jersey

Ngah WSW, Hanafiah MAKM (2008) Biosorption of copper ions from dilute aqueous solutions on base treatedrubber (Hevea brasiliensis) leaves powder: kinetics, isotherm, and biosorption mechanisms. J Environ Sci 20:1168–1176. https://doi.org/10.1016/S1001-0742(08)62205-6

Nishikawa E, Neto AFA, Vieira MGA (2012) Equilibrium and thermodynamic studies of zinc adsorption on expanded vermiculite. Adsorpt Sci Technol 30:759–772. https://doi.org/10.1260/0263-6174.30.8-9.759

Panuccio MR, Sorgonà A, Rizzo M, Cacco G (2009) Cadmium adsorption on vermiculite, zeolite and pumice: batch experimental studies. J Environ Manage 90:364–374. https://doi.org/10.1016/j.jenvman.2007.10.005

Park CM, Kim YM, Kim K-H et al (2019) Potential utility of graphene-based nano spinel ferrites as adsorbent and photocatalyst for removing organic/inorganic contaminants from aqueous solutions: a mini review. Chemosphere 221:392–402. https://doi.org/10.1016/j.chemosphere.2019.01.063

Paula RF (2014) Vermiculita. In: DNPM, vol 34. Sumário Mineral, Brasília, pp 122–123

Puigdomenech I (2010) Chemical equilibrium diagrams. Hydra/Medusa. Inorganic Chemistry Royal Institute of Technology (KTH), Sweden

Rahman MS, Sathasivam KV (2015) Heavy metal adsorption onto Kappaphycus sp. from aqueous solutions: the use of error functions for validation of isotherm and kinetics models. Biomed Res Int 2015:1–13. https://doi.org/10.1155/2015/126298

Rajendran S, Priya AK, Senthil Kumar P et al (2022) A critical and recent developments on adsorption technique for removal of heavy metals from wastewater-a review. Chemosphere 303:135146. https://doi.org/10.1016/j.chemosphere.2022.135146

Ruthven DM (1984) Principles of adsorption and adsorption processes. John Wiley & Sons, New York, NY

Saha P, Chowdhury S (2011) Insight into adsorption thermodynamics. In: Thermodynamics. InTech

Souza Santos P (1975) Ciência e Tecnologia de Argilas, Aplicada às Argilas Brasileiras e Aplicações, vol 1–2. Edgar Blücher, Sao Paulo

Sutcu M (2015) Influence of expanded vermiculite on physical properties and thermal conductivity of clay bricks. Ceram Int 41:2819–2827. https://doi.org/10.1016/j.ceramint.2014.10.102

Tran HN, You S-J, Chao H-P (2016) Thermodynamic parameters of cadmium adsorption onto orange peel calculated from various methods : a comparison study. J Environ Chem Eng 4:2671–2682. https://doi.org/10.1016/j.jece.2016.05.009

Wadhawan S, Jain A, Nayyar J, Mehta SK (2020) Role of nanomaterials as adsorbents in heavy metal ion removal from waste water: a review. J Water Process Eng 33:101038. https://doi.org/10.1016/j.jwpe.2019.101038

World Health Organization (WHO) (2017) Guidelines for drinking-water quality, 4th edn. WHO Press, Geneva. https://doi.org/10.1016/S1462-0758(00)00006-6

Xu W, Liu C, Zhu J-M et al (2022) Adsorption of cadmium on clay-organic associations in different pH solutions: the effect of amphoteric organic matter. Ecotoxicol Environ Saf 236:113509. https://doi.org/10.1016/j.ecoenv.2022.113509

Yu Y, Zhuang Y-Y, Wang Z-H (2001) Adsorption of water-soluble dye onto functionalized resin. J Colloid Interface Sci 242:288–293. https://doi.org/10.1006/jcis.2001.7780

Zhou Q, Liu Y, Li T et al (2020) Cadmium adsorption to clay-microbe aggregates: implications for marine heavy metals cycling. Geochim Cosmochim Acta 290:124–136. https://doi.org/10.1016/j.gca.2020.09.002